

## Cu(II) Adsorption from Aqueous Solution Using K<sub>2</sub>CO<sub>3</sub>-Activated Carbon Derived from *Chenopodium botrys*: A Sustainable Approach

Selma EKİNCİ<sup>1</sup>, Erhan ONAT<sup>2</sup>, Ramazan ASTAN<sup>3</sup>

<sup>1</sup> Vocational School of Technical Sciences, Department of Chemistry and Chemical Process Technology, Batman University, Batman, Turkey

<sup>2</sup> Vocational School of Organized Industrial Zone, Department of Electrical and Energy, Bitlis Eren University, Bitlis, Turkey

<sup>3</sup>Postgraduate Education Institute, Batman University, Batman, Turkey

✉: [selma.ekinci@batman.edu.tr](mailto:selma.ekinci@batman.edu.tr)  [0000-0002-7835-4832](https://orcid.org/0000-0002-7835-4832)  [0000-0003-1638-0151](https://orcid.org/0000-0003-1638-0151)  [0009-0002-6516-0411](https://orcid.org/0009-0002-6516-0411)

Received (Geliş): 05.03.2025

Revision (Düzeltilme): 07.04.2025

Accepted (Kabul): 25.04.2025

### ABSTRACT

This study investigates the adsorption performance of a novel activated carbon synthesized from *Chenopodium botrys* using potassium carbonate (K<sub>2</sub>CO<sub>3</sub>) for the removal of Cu(II) ions. The structural and surface properties of the prepared adsorbent were characterized by FT-IR, SEM, and EDX analyses, confirming its porous structure and the presence of surface functional groups. Adsorption experiments were conducted to determine the optimum operating conditions, and kinetic data showed a strong fit to the pseudo-second-order model, indicating that the process is governed by chemisorption. Isotherm analysis revealed that the adsorption occurred in multilayers on a heterogeneous surface, with the Freundlich model providing the best fit. Thermodynamic evaluations demonstrated the endothermic nature of the process, with adsorption capacity increasing with temperature. Overall, the results suggest that this *Chenopodium botrys*-derived activated carbon is a cost-effective and environmentally friendly material for the treatment of Cu(II)-contaminated wastewater.

**Keywords:** Adsorption, Activated carbon, *Chenopodium botrys*, Removal of Cu (II), Heavy metal

## Chenopodium botrys'ten Türetilen K<sub>2</sub>CO<sub>3</sub>-Aktif Karbon Kullanılarak Sulu Çözeltiden Cu(II) Adsorpsiyonu: Sürdürülebilir Bir Yaklaşım

### ÖZ

Bu çalışma, *Chenopodium botrys* bitkisinden potasyum karbonat (K<sub>2</sub>CO<sub>3</sub>) kullanılarak sentezlenen yeni bir aktif karbonun Cu(II) iyonlarının giderimindeki adsorpsiyon performansını araştırmaktadır. Üretilen adsorbanın yapısal ve yüzey özellikleri FT-IR, SEM ve EDX analizleri ile karakterize edilmiş; gözenekli yapısı ve yüzey fonksiyonel gruplarının varlığı doğrulanmıştır. Adsorpsiyon deneyleriyle optimum çalışma koşulları belirlenmiş ve kinetik veriler, sürecin kimyasal adsorpsiyonla gerçekleştiğini gösteren sözde ikinci dereceden modele yüksek uyum sağlamıştır. İzoterm analizleri, adsorpsiyonun heterojen yüzeylerde çok katmanlı gerçekleştiğini ve Freundlich modeli ile en iyi şekilde tanımlandığını ortaya koymuştur. Termodinamik analizler, sürecin endotermik karakterde olduğunu ve sıcaklık artışıyla adsorpsiyon kapasitesinin yükseldiğini göstermiştir. Elde edilen sonuçlar, *Chenopodium botrys* kökenli bu aktif karbonun, Cu(II) içeren atık suların arıtımında ekonomik ve çevre dostu bir alternatif olabileceğini göstermektedir.

**Anahtar Kelimeler:** Adsorpsiyon, Aktif karbon, *Chenopodium botrys*, Cu (II), Ağır metal

### INTRODUCTION

Heavy metal pollution in water bodies has emerged as a major environmental and public health concern due to its toxicity and persistence [1-4]. Among various heavy metals, Cu(II) is widely recognized for its hazardous effects when present in excessive amounts [5-7]. Industrial activities such as electroplating, mining, and fertilizer production contribute significantly to copper contamination in water [8,9]. The accumulation of Cu(II) in aquatic systems poses risks including bioaccumulation

in marine organisms and long-term health issues in humans, such as liver and kidney damage, neurological disorders, and gastrointestinal distress [10,11]. Therefore, the development of efficient, cost-effective, and environmentally sustainable methods for Cu(II) removal is essential [12].

Adsorption is widely considered one of the most effective techniques for heavy metal removal due to its simplicity, high efficiency, and low operational costs [13]. Activated carbon, known for its large surface area and porosity, is a preferred adsorbent. The selection of precursor

materials for activated carbon production significantly influences its adsorption capacity and economic feasibility [14,15]. In recent years, agricultural and plant-based wastes have gained attention as sustainable and renewable precursors for activated carbon synthesis [16-21].

Chenopodium botrys, commonly known as Jerusalem oak, is an underutilized plant species with a high carbon content, making it a promising raw material for activated carbon production. This study utilizes Chenopodium botrys as a precursor for activated carbon synthesis, employing  $K_2CO_3$  as a chemical activator to enhance surface area and porosity. The prepared activated carbon was evaluated for Cu(II) adsorption under different experimental conditions to determine its efficiency and adsorption mechanism [22-24]. The study further investigates the adsorption kinetic, and isotherm properties to provide insights into the adsorption process. This study gives light on the adsorption mechanisms and emphasizes the potential of  $K_2CO_3$ -activated carbon as a sustainable heavy metal removal solution by examining the adsorption behavior of Cu(II) on Chenopodium botrys-derived activated carbon and evaluating the kinetic and isotherm parameters.

## MATERIAL and METHODS

### Preparation of Chenopodium botrys

Chenopodium botrys was harvested from fields in Bitlis and dried at room temperature for 30 days. The dried material was thoroughly washed with deionized water, ground, and sieved to obtain particles of 300–500  $\mu\text{m}$ . The sample was then heated at 105  $^\circ\text{C}$  for 24 hours to eliminate residual moisture and stored in a sealed container under laboratory conditions.

### Preparation method of activated carbon

Activated carbon was synthesized using chemical activation with  $K_2CO_3$ . A 1:1 ratio of organic matter to  $K_2CO_3$  was used, where 5 g of Chenopodium botrys and 5 g of  $K_2CO_3$  were mixed with 50 mL of deionized water and left for impregnation for 24 hours. The mixture was then filtered and subjected to carbonization in a high-purity  $N_2$  atmosphere at 500  $^\circ\text{C}$  for 45 minutes. After activation, the sample was washed with 0.5 M HCl to remove residual impurities, followed by multiple rinses with boiling deionized water. The final product was dried at 120  $^\circ\text{C}$  for 12 hours.

### Adsorption experiments

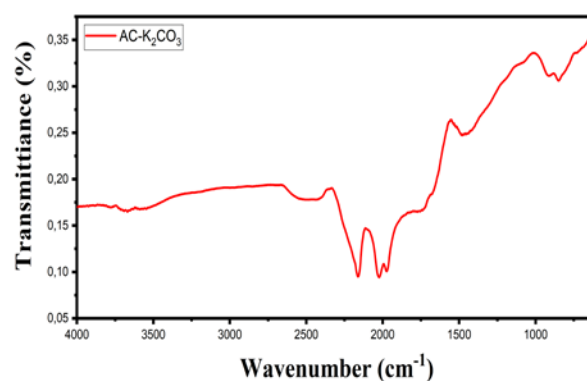
A series of erlenmeyer flasks with a 50 mL volume were used for these studies. By choosing pH, concentration, adsorbent quantity, and contact time, the factors influencing adsorption were experimentally examined. A 1000 ppm stock solution of Cu (II) ions was prepared with  $Cu(SO_4).5H_2O$ . Cu (II) ion solutions ranging from 25 to 150 ppm were prepared by dilution from the stock

solution and utilized for isotherm investigations. Then the measurements were made at room temperature at specific pH values (2-10). In each experimental series, the process was conducted in accordance with the proper contact time after 50 mL of metal solution and the correct volumes of activated carbon were combined in a shaker running at 10,000 rpm. Following adsorption, the samples were filtered, and a UV-Vis spectrometer was used to determine copper amount in the supernatant.

## RESULTS and DISCUSSION

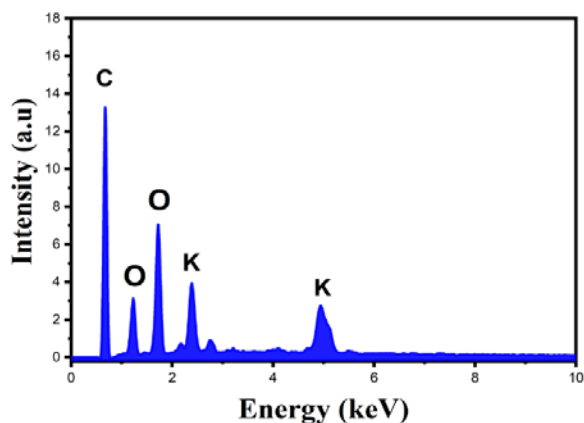
### Characterization of activated carbon with FT-IR, EDX, and SEM

The FT-IR spectrum of activated carbon produced through  $K_2CO_3$  activation, as shown in Figure 1, offers valuable information about the adsorbent surface. The transmittance spectrum displays distinct peaks at specific wavenumbers, corresponding to various chemical bonds and functional groups. A broad band in the 3400–3600  $\text{cm}^{-1}$  range is typically associated with O–H stretching vibrations, which may arise from adsorbed moisture or hydroxyl groups attached to the surface. The presence of these hydroxyl groups suggests potential hydrogen bonding interactions that enhance the adsorption properties of the material [4]. C=O stretching vibrations are represented by a noticeable absorption band at about 1700  $\text{cm}^{-1}$ , which suggests the existence of carboxyl or carbonyl functional groups. These oxygen-containing groups play a significant role in adsorption mechanisms, especially in the removal of metal ions [25,26]. C=C stretching vibrations from aromatic compounds inside the carbon matrix are responsible for peaks in the 1500–1600  $\text{cm}^{-1}$  range, which validate the synthesis of activated carbon [27]. Furthermore, bands seen between 1000 and 1300  $\text{cm}^{-1}$  are linked to ether, lactone, or phenol groups' C–O stretching vibrations. These functional groups contribute to adsorption by providing active sites for interactions with pollutants [28].



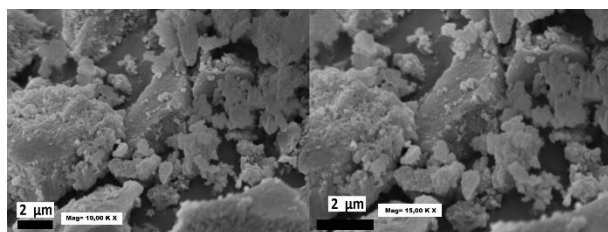
**Figure 1.** FT-IR analysis of Chenopodium botrys-activated carbon.

The EDX spectrum in Figure 2 confirms that the sample contains primarily carbon (C), with notable amounts of oxygen (O) and potassium (K). The oxygen signals indicate that the carbon structure may have oxygen-containing functional groups, enhancing chemical reactivity. The presence of potassium suggests that some K from the activation agent ( $K_2CO_3$ ) remains, which may affect the material's properties. This composition is typical for activated carbon prepared using alkali activation, commonly used for adsorption, catalysis, and electrochemical applications.



**Figure 2.** EDX analysis of activated carbon derived from *Chenopodium botrys*

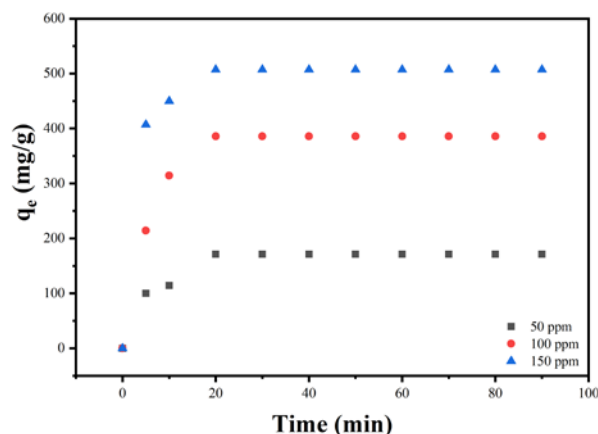
The SEM images in Figure 3 show an irregular, porous, and rough surface, characteristic of activated carbon. The sample consists of aggregated carbon particles with varying sizes, some larger chunks mixed with finer particles. The rough texture suggests significant surface modifications, likely due to the activation process. The presence of numerous micro- and mesoporous is visible as small cavities and rough edges.  $K_2CO_3$  activation is known to create well-developed porosity by chemical etching, which enhances the surface area for adsorption. The particles appear loosely packed, with some forming agglomerates. The fine powder-like structures indicate that the material may have undergone fragmentation during the activation or post-processing. The activation process with  $K_2CO_3$  leads to carbon gasification and pore formation, which enhances the porosity. The rough and uneven structure indicates that  $K_2CO_3$  effectively created micropores.



**Figure 3.** SEM analysis of *Chenopodium botrys*-activated carbon.

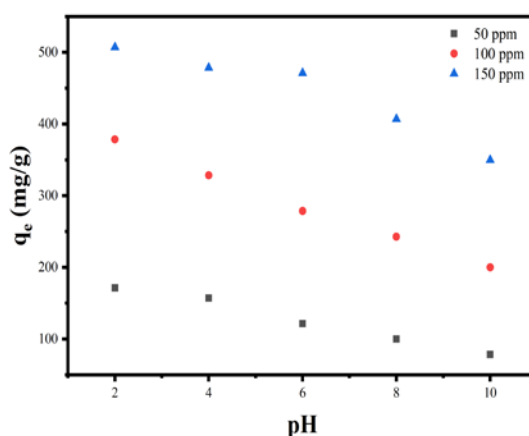
**Optimum adsorption conditions**

In Figure 4, for all concentrations, the adsorption capacity increases quickly within the first 20 minutes, suggesting fast surface adsorption. After 20 minutes, the adsorption capacity plateaus, indicating that equilibrium has been reached. Adsorption sites are saturated, and further Cu(II) removal slows down significantly at equilibrium.



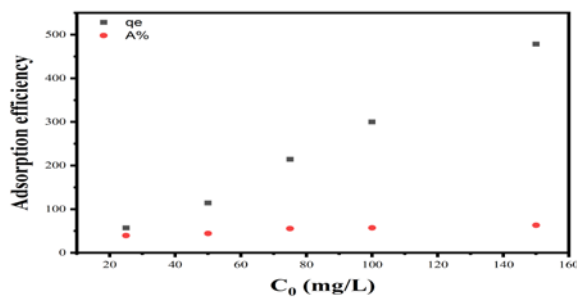
**Figure 4.** The effect of contact time on the adsorption of Cu (II) ions by *Chenopodium botrys*-activated carbon.

Figure 5 shows that Cu(II) adsorption is strongly pH-dependent, with maximum adsorption occurring at pH 2. At low pH, adsorption is at its highest for all concentrations. As pH increases beyond pH 6, adsorption capacity gradually decreases. This trend is consistent across all Cu(II) concentrations. At low pH levels, negatively charged  $Cu^{+2}$  forms are electrostatically bonded to the positively charged adsorbent surface due to the abundance of hydrogen ions in the surrounding environment. Reference studies have reported similar findings [29,30].



**Figure 5.** The effect of pH on the adsorption of Cu (II) ions by *Chenopodium botrys*-activated carbon

According to Figure 6, as the initial Cu(II) concentration increases from 25 to 150 mg/L, the adsorption capacity ( $q_e$ ) steadily increases. This suggests that more Cu(II) ions are available in solution, leading to higher adsorption per gram of adsorbent. The percentage removal of Cu(II) decrease as  $C_0$  increases. At low initial concentrations, A% is higher, indicating efficient adsorption due to the availability of abundant active sites. At concentrations above 100 mg/L, A% decreases, suggesting that adsorption sites are approaching saturation [31].



**Figure 6.** The effect of initial concentration on the adsorption of Cu (II) ions by Chenopodium botrys-activated carbon

At low adsorbent dosages (0.01 g),  $q_e$  is highest for all concentrations (Figure 7). At 150 ppm, adsorption capacity is the highest across all adsorbent dosages, followed by 100 ppm and 50 ppm. This suggests that more Cu(II) ions are available in solution, leading to higher uptake per gram of adsorbent. Increasing adsorbent dosage increases the number of available adsorption sites, but at the same time, the Cu(II) concentration remains the same. Since the ratio of available metal ions to adsorbent sites decreases, the adsorption capacity ( $q_e$ ) per gram of adsorbent declines. While the total amount of Cu(II) removed increases with adsorbent dose, the adsorption per gram of adsorbent decreases. This is because, at higher dosages, excess adsorption sites remain unused, leading to lower adsorption efficiency per gram [32,33].

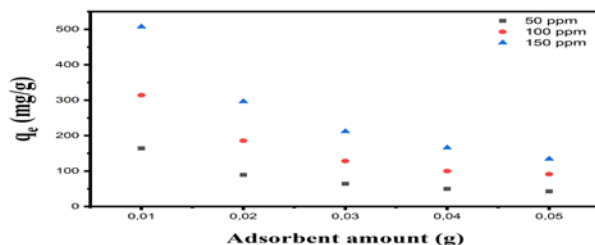


**Figure 7.** The effect of adsorbent amount on the adsorption of Cu (II) ions by Chenopodium botrys-activated carbon

### Adsorption's kinetic way

The linear form of the pseudo-first-order (PFO) and pseudo-second-order (PSO) kinetic models is expressed by equations 1 and 2, respectively.

$$\log(q_e - q) = \log q_e - \frac{k_1}{2.303} \cdot t \quad (1)$$

$$\frac{t}{q} = \frac{1}{k_2 q_e^2} + \frac{1}{q_e} t \quad (2)$$

By drawing graphs of the given linear form of equations,  $k_1$ ,  $k_2$  and  $q_e$  values were obtained using the line's slope and slip values. Fig. 8, 9 and the kinetic data in the Table 1 provide insights into the adsorption behavior of Cu (II) ions on activated carbon derived from Chenopodium botrys. Based on the given kinetic parameters, we can evaluate the adsorption process from a kinetic perspective. The PFO rate constant ( $k_{ads,1}$ ) decreases as the initial concentration increases (from 0.0468 to 0.1122  $\text{min}^{-1}$ ), suggesting that adsorption is initially rapid but slows down at higher concentrations. The  $q_{e,exp}$  (experimental adsorption capacity) values are significantly higher than the  $q_{e,cal}$  values indicating that the PFO model does not perfectly fit the adsorption process. The determination coefficient ( $R^2$ ) values for the PFO model are high ( $\geq 0.9989$ ), indicating a reasonably good fit but not the best compared to the PSO model. The PSO rate constant ( $k_{ads,2}$ ) decreases with increasing concentration (from  $1,9 \cdot 10^{-3}$  to  $2,3 \cdot 10^{-3}$ ), suggesting that chemical interactions between Cu (II) and the adsorbent become more dominant at higher concentrations. The calculated adsorption capacity ( $q_{e,cal}$ ) values are much closer to the experimental values ( $q_{e,exp}$ ), which indicates that the PSO model better represents the adsorption kinetics. The  $R^2$  values for the PSO model are very high ( $\geq 0.9976$ ), confirming that the adsorption process follows PSO kinetics more closely. The adsorption of Cu (II) ions onto activated carbon follows PSO kinetics rather than PFO kinetics. This suggests that the adsorption process is primarily controlled by chemisorption, involving electron sharing or exchange between the adsorbent and adsorbate. The increasing trend in  $q_{e,exp}$  with concentration suggests that adsorption sites are not fully saturated, and higher concentrations lead to greater adsorption. The decrease in  $k_{ads,2}$  with concentration implies that adsorption sites become more occupied, reducing the availability of active sites for new Cu (II) ions. Thus, the kinetic evaluation suggests that chemisorption is the dominant mechanism governing the adsorption of Cu (II) ions onto the activated carbon derived from Chenopodium botrys.

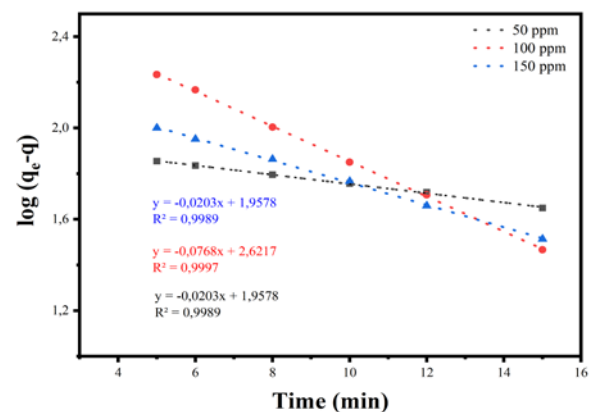


**Figure 8.** The PFO kinetic equation drawings of the adsorption

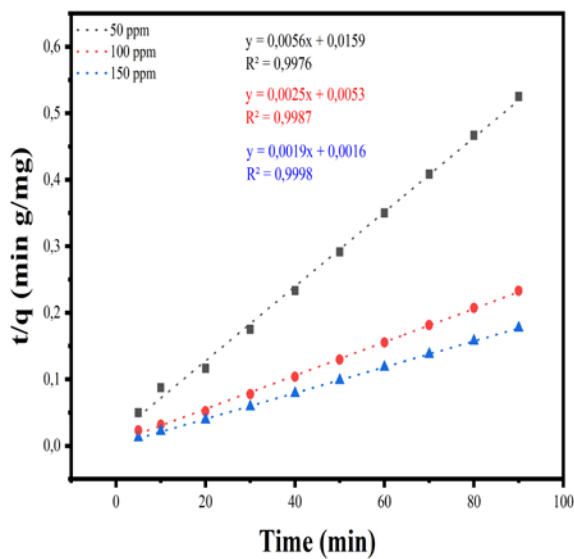


Figure 9. The PSO kinetic equation drawings of the adsorption

Table 1. Kinetic parameters of adsorption of Cu (II) on activated carbon derived from Chenopodium Botrys.

Concentration (ppm)	PFO model			
	$k_{ads,1}$ (min <sup>-1</sup> )	$q_{e,exp}$ (mg g <sup>-1</sup> )	$q_{e,cal}$ (mg g <sup>-1</sup> )	R <sup>2</sup>
50	0,0468	171,4	90,74	0,9989
100	0,1769	385,7	418,5	0,9997
150	0,1122	507,15	176,69	0,9992

Concentration (ppm)	PSO model		
	$k_{ads,2}$ (g mg <sup>-1</sup> min <sup>-1</sup> )	$q_{e,cal}$ (mg g <sup>-1</sup> )	R <sup>2</sup>
50	1,9.10 <sup>-3</sup>	178,57	0,9976
100	1,2.10 <sup>-3</sup>	400	0,9987
150	2,3.10 <sup>-3</sup>	526,32	0,9998

### Freundlich isotherm model

Although the experimental data were evaluated using the linear equations of both the Langmuir (LI) and Freundlich isotherms (FI) (Equ.3), the results were only fitted to the FI model (Figure 10). Accordingly, it can be concluded that the adsorption occurs on a heterogeneous surface and the adsorption is strong because the n value is less than 1.

$$\log q_e = \log k + \frac{1}{n} \log C_e \quad (3)$$

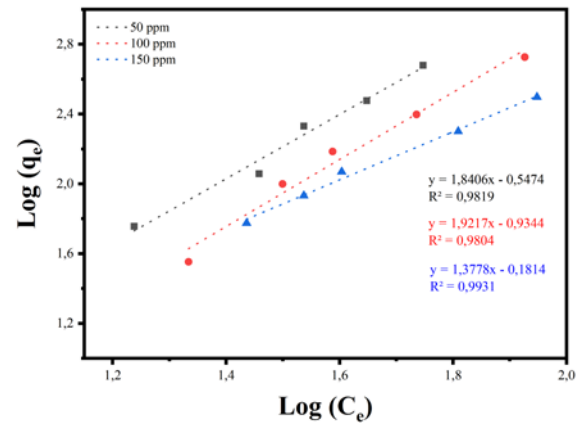


Figure 10. The linear drawings of Freundlich isotherm model of the adsorption

The data in the Table 2 presents the FI constants (k and n) for the adsorption of Cu(II) ions on activated carbon at different temperatures. Since the LI model does not fit the experimental data, it can be concluded that adsorption does not occur on a homogeneous surface with monolayer adsorption; instead, the FI model suggests multilayer adsorption on a heterogeneous surface. The increase in “k” constants with temperature suggests an endothermic process, meaning adsorption efficiency improves at higher temperatures.

The adsorption of Cu(II) onto activated carbon follows a PSO kinetic model, indicating chemisorption as the dominant mechanism. However, the isotherm data fits the FI model, suggesting multilayer adsorption on a heterogeneous surface rather than monolayer adsorption. This implies a two-stage process: initial physisorption through weak interactions, followed by chemisorption at high-energy sites via surface complexation or ion exchange. The increasing adsorption capacity with temperature further supports the involvement of chemisorption. Overall, the process can be described as heterogeneous chemisorption, where strong chemical interactions dominate, but weaker physical interactions also contribute.

Table 2 FI model parameters for adsorption

Temperature (K)	FI model		
	k	n	R <sup>2</sup>
298	0,2835	0,5433	0,9819
308	0,361	0,623	0,9804
318	0,6586	0,7258	0,9931

### CONCLUSION

This study successfully synthesized activated carbon

from *Chenopodium botrys* using  $K_2CO_3$  activation and demonstrated its effectiveness for Cu(II) removal. The physicochemical characterization of the prepared activated carbon revealed a well-developed porous structure with abundant functional groups. The presence of hydroxyl, carboxyl, and aromatic functional groups contributed to enhanced adsorption performance by providing active binding sites for Cu(II) ions. The adsorption process was systematically evaluated under different conditions. Adsorption experiments showed that Cu(II) removal was pH-dependent, with maximum adsorption occurring at pH 2. Adsorption equilibrium was rapidly attained within the first 20 minutes, indicating a high affinity between the activated carbon's surface and Cu(II) ions. As the initial Cu(II) concentration rose, the adsorption capacity rose as well, but the % removal fell, indicating that the accessible adsorption sites were gradually saturated. Furthermore, because there were more active sites present at larger adsorbent dosages, the adsorption capacity per gram of adsorbent dropped.

Indicating that chemisorption was a major factor in Cu(II) uptake, kinetic modeling revealed that the adsorption process followed a PSO kinetic model. The experimental data was best fitted by the FI model, which showed multilayer adsorption over a heterogeneous surface. The endothermic character of the process was proved by the increasing FI constant (k) with temperature, suggesting that higher temperatures improved adsorption efficiency.

Overall, the findings demonstrate the potency of activated carbon generated from *Chenopodium botrys* as a sustainable and efficient material for the uptake of Cu(II).

## ACKNOWLEDGEMENTS

This study was derived from Ramazan ASTAN's master's thesis.

## REFERENCES

- [1] Zamora-Ledezma C., Negrete-Bolagay D., Figueroa F., Zamora-Ledezma E., Ni M., Alexis F., Guerrero V. Heavy metal water pollution: A fresh look about hazards, novel and conventional remediation methods, *Environmental Technology & Innovation*. 22 101504, 2012. <https://doi.org/10.1016/J.ETI.2021.101504>
- [2] Kumar V., Parihar R., Sharma A., Bakshi P., Sidhu G., Bali A., Karaouzias I., Bhardwaj R., Thukral A., Gyasi-Agyei Y., Rodrigo-Comino J. Global evaluation of heavy metal content in surface water bodies: A meta-analysis using heavy metal pollution indices and multivariate statistical analyses, *Chemosphere*. 236 124364, 2019. <https://doi.org/10.1016/j.chemosphere.2019.124364>
- [3] Aziz K., Mustafa F., Omer K., Hama S., Hamarawf R., Rahman K. Heavy metal pollution in the aquatic environment: efficient and low-cost removal approaches to eliminate their toxicity: a review, *RSC Advances*. 13 17595–17610, 2023. <https://doi.org/10.1039/d3ra00723e>
- [4] Ekinci S., Onat E., Atiç S. Optimized synthesis and characterization of activated carbon from corn silk and corn silk hydrochar, *ChemistrySelect*. 10(5) e202405854, 2025. <https://doi.org/10.1002/slct.202405854>
- [5] Ekinci S., Onat E. Activated carbon assisted cobalt catalyst for hydrogen production: synthesis and characterization, *Balıkesir Üniversitesi Fen Bilimleri Enstitüsü Dergisi*. 26(2) 455-471, 2024. <https://doi.org/10.25092/baunfbd.1297146>
- [6] Smriti A.A., Lodhi A., Shukla S. Copper toxicity in aquatic ecosystem: A Review, *International Journal of Fisheries and Aquatic Studies*. 11(4) 134-138, 2023. <https://doi.org/10.22271/fish.2023.v11.i4b.2835>
- [7] Liu Y., Wang H., Cui Y., Chen N. Removal of Copper Ions from Wastewater: A Review, *International Journal of Environmental Research and Public Health*. 20(5) 3885, 2023. <https://doi.org/10.3390/ijerph20053885>
- [8] Comber S., Deviller G., Wilson I, Peters A, Merrington G, Borrelli P, Baken S. (2022). Sources of copper into the European aquatic environment, *Integrated Environmental Assessment and Management*. 19(4) 1031–1047, 2023. <https://doi.org/10.1002/ieam.4700>
- [9] Krayem M., Khatib S., Hassan Y., Deluchat V., Labrousse P. In search for potential biomarkers of copper stress in aquatic plants, *Aquatic Toxicology*. 239 105952, 2021. <https://doi.org/10.1016/j.aquatox.2021.105952>
- [10] Castaldo G., Flipkens G., Pillet M., Town R., Bervoets L., Blust R., Boeck G. Antagonistic bioaccumulation of waterborne Cu(II) and Cd(II) in common carp (*Cyprinus carpio*) and effects on ion-homeostasis and defensive mechanisms, *Aquatic Toxicology*. 226 105561, 2020. <https://doi.org/10.1016/j.aquatox.2020.105561>
- [11] Keller A., Adeleye A., Conway J., Garner K., Zhao L., Cherr G., Hong J., Gardea-Torresdey J., Godwin H., Hanna S., Ji Z., Kaweeteerawat C., Lin S., Lenihan H.M., et al. Comparative environmental fate and toxicity of copper nanomaterials, *NanoImpact*. 7 28-40, 2017. <https://doi.org/10.1016/J.IMPACT.2017.05.003>
- [12] Tumamos S., Ensano B., Pingul-Ong S., Ong D., Kan C., Yee J., De Luna M. Isotherm, kinetics and thermodynamics of Cu(II) and Pb(II) adsorption on groundwater treatment sludge-derived manganese dioxide for wastewater treatment Applications, *International Journal of Environmental Research and Public Health*. 18(6) 3050, 2021; <https://doi.org/10.3390/ijerph18063050>
- [13] Onat E., Ekinci S., A new material fabricated by the combination of natural mineral perlite and graphene oxide: Synthesis, characterization, and methylene blue removal, *Diamond and Related Materials*. 143 110848, 2024. <https://doi.org/10.1016/j.diamond.2024.110848>
- [14] Adame-Pereira M., Durán-Valle C., Fernández-González C.. Hydrothermal carbon coating of an activated carbon—A new adsorbent, *Molecules*. 28(12) 4769, 2023. <https://doi.org/10.3390/molecules28124769>
- [15] Wang X., Cheng H., Ye G., Fan J., Yao F., Wang Y., Jiao Y., Zhu W., Huang H., Ye D. Key factors and primary modification methods of activated carbon and their application in adsorption of carbon-based gases: A review, *Chemosphere*. 287(2) 131995, 2021. <https://doi.org/10.1016/j.chemosphere.2021.131995>
- [16] Ukanwa K., Patchigolla K., Sakrabani R., Anthony E., Mandavgane S. A review of chemicals to produce activated carbon from agricultural waste biomass, *Sustainability*. 11(22) 6204, 2019. <https://doi.org/10.3390/su11226204>
- [17] Blachnio M., Deryło-Marczewska A., Charmas B., Zienkiewicz-Strzałka M., Bogatrov V., Galaburda M. Activated carbon from agricultural wastes for adsorption of organic pollutants, *Molecules*. 25(21) 5105, 2020. <https://doi.org/10.3390/molecules25215105>
- [18] Nazem M., Zare M., Shirazian S. Preparation and optimization of activated nano-carbon production using physical activation by water steam from agricultural wastes, *RSC Advances*. 10,1463 – 1475, 2020. <https://doi.org/10.1039/c9ra07409k>
- [19] Wu H., Chen S., Liao W., Wang W., Jang M., Chen W., Ahamad T., Alshehri S., Hou C., Lin K., Charinpanitkul T., Wu K. Assessment of agricultural waste-derived activated carbon in multiple applications, *Environmental Research*. 191 110176, 2020. <https://doi.org/10.1016/j.envres.2020.110176>
- [20] Lewoyehu M. Comprehensive review on synthesis and application of activated carbon from agricultural residues for the

- remediation of venomous pollutants in wastewater, *Journal of Analytical and Applied Pyrolysis*. 159 105279, 2021. <https://doi.org/10.1016/J.JAAP.2021.105279>
- [21] Kosheleva R., Mitropoulos A., Kyzas G. Synthesis of activated carbon from food waste, *Environmental Chemistry Letters*. 17 429-438, 2018. <https://doi.org/10.1007/s10311-018-0817-5>
- [22] Bojilov D., Manolov S., Nacheva A., Dagnon S., Ivanov I. Characterization of polyphenols from chenopodium botrys after fractionation with different solvents and study of their in vitro biological activity, *Molecules*. 28(12) 4816, 2023. <https://doi.org/10.3390/molecules28124816>
- [23] Gupta N., Sagar R., Kori M. Hepatoprotective potential of methanolic and aqueous extract of chenopodium botrys against lead-induced toxicity, *International Journal of Pharmaceutical Investigation*. 11(2) 165-169, 2021. <https://doi.org/10.5530/IJPI.2021.2.30>
- [24] Sezer E., Uysal T. Phenolic screening and biological activities of *Chenopodium botrys* L. extracts, *Anatolian Journal of Botany*. 5(2) 78-83, 2021. <https://doi.org/10.30616/AJB.890324>
- [25] Wang L., Sun F., Hao F., Qu Z., Gao J., Liu M., Wang K., Zhao G., Qin Y. A green trace  $K_2CO_3$  induced catalytic activation strategy for developing coal-converted activated carbon as advanced candidate for  $CO_2$  adsorption and supercapacitors, *Chemical Engineering Journal*. 383 123205, 2020. <https://doi.org/10.1016/j.cej.2019.123205>
- [26] Peter O., Adeyinka O., Akolade R. Application of snail shell chitosan as a bioadsorbent in removal of copper (II) ions from wastewater, *Earthline Journal of Chemical Sciences*. 2(1) 141-151, 2019. <https://doi.org/10.34198/EJCS.2119.141151>
- [27] Cheng X., Wei M., Tian G., Luo Y., Hua W. Vibrationally-resolved X-ray photoelectron spectra of six polycyclic aromatic hydrocarbons from first-principles simulations, *The Journal of Physical Chemistry A*. 126(33) 5582-5593, 2022. <https://doi.org/10.1021/acs.jpca.2c04426>
- [28] Hong T., Yin J.Y., Nie S.P., Xie M.Y. Applications of infrared spectroscopy in polysaccharide structural analysis: Progress, challenge and perspective, *Food Chemistry: X*. 12 100168, 2021. <https://doi.org/10.1016/j.fochx.2021.100168>
- [29] Torrellas S.A., Lovera R.G., Escalona N., Sepúlveda C., Sotela J.L., Garcia J. Chemical-activated carbons from peach stones for the adsorption of emerging contaminants in aqueous solutions, *Chemical Engineering Journal*. 279 788-798, 2015. <http://dx.doi.org/10.1016/j.cej.2015.05.104>
- [30] Gezer B. Cu (II) adsorption with activated carbon obtained from sea urchin prepared by ultrasound-assisted method, *Nigde Omer Halisdemir University Journal of Engineering Sciences*, 9(2) 770-780, 2020. <https://doi.org/10.28948/ngumuh.700773>
- [31] Ekinçi S. Production of hydrochar from corn silk by hydrothermal carbonization technique and its modification for more effective removal of Cr (VI). *Journal of Chinese Chemical Society*. 71(1) 84-98, 2024. <https://doi.org/10.1002/jccs.202300342>
- [32] Ekinçi S. Elimination of methylene blue from aqueous medium using an agricultural waste product of crude corn silk (*Stylus maydis*) and corn silk treated with sulphuric acid, *ChemistrySelect*. 8(18) e202300284, 2023. <https://doi.org/10.1002/slct.202300284>
- [33] Onat E., Ekinçi S. Investigation of chromium (VI) heavy metal removal from water using activated carbon produced by hydrothermal pretreatment from industrial waste. In book: *Science and Mathematics in a Globalizing World*. Duvar Publishing, pp:45-61, April 2023.